RAL-85-052

Science and Engineering Research Council
Rutherford Appleton Laboratory
CHILTON, DIDCOT, OXON, OX11 0QX

RAL-85-052

MARS - A Multi-Angle Rotor Spectrometer for the SNS

C J Carlile, A D Taylor and W G Williams

June 1985

Spallation Neutron Source

Description of Accelerator and Target

Edited by B. Boardman

March 1982

RAL-82-006

RAL-85-052

MARS - A MULTI-ANGLE ROTOR SPECTROMETER FOR THE SNS.

C J Carlile, A D Taylor and W G Williams.

Abstract

The design concept for an optimised direct geometry inelastic spectrometer on the SNS is discussed with the emphasis on the choice of the monochromating method. The resolutions, dynamic ranges and fluxes achievable with crystals and phased choppers are calculated for the incident energy range $20 \leq E_1$ (meV) ≤ 500. We also consider the practicalities of realising a spectrometer to provide 1% energy transfer resolutions over a large (Q,ε) range. It is shown that the chopper spectrometer is the better choice for the major part of this incident energy range, but that the crystal method, particularly in a double monochromator arrangement, may offer advantages at the lowest energies. While anticipating that most applications will require the rotor option we consider that the most versatile spectrometer is a hybrid one, and make recommendations on a suitable spectrometer design.

Inelastic Scattering Group
Neutron Division
June 1985

1. INTRODUCTION

Direct geometry time-of-flight inelastic neutron scattering spectrometers have long been used on steady state sources to measure the dynamical structure factor and frequency distribution of isotropic systems. The scientific interest [1] in such spectrometers comes from fields as diverse as excitations in solids, liquids, amorphous and disordered systems, magnetic scattering and molecular spectroscopy. In this paper we discuss the characteristics of the equivalent pulsed source spectrometer and show that an advanced spallation source such as SNS [2] may be used to improve the resolution and expand the kinematic range available. Such a spectrometer must cover a wide and variable region of Q-ε space. This may be achieved by a versatile monochromating device capable of providing a variety of incident energies at an appropriate high resolution, say 1%, and a wide but closely spaced set of scattering angles.

The provision of an inelastic neutron scattering spectrometer which specialises in measuring energy transfers in the thermal energy range (10 - 150 meV) has always been considered as essential in a full suite of instruments on the SNS. Such a spectrometer was identified in the original report which put forward the scientific case for the SNS [3] as one of 26 instruments requiring further study with a view to its installation at the SNS. Three of the four working groups of the SNS Science Panel (Solid State Physics, Fluids and Amorphous Solids and Molecular and Biological Sciences) endorsed the need for a 'Moderate' Energy Transfer Spectrometer, with an energy transfer capability $0 \leqslant \varepsilon \leqslant 200$ meV with energy resolutions of 1 or 2 percent. A large and continuous range of momentum transfer Q was requested; measurements at low Q were considered to be important but only at modest Q resolutions ($\Delta Q/Q \sim 5\%$). Two of the working groups identified the need for polarisation analysis. The spectrometer was specified as a direct geometry time of flight instrument using as the monochromator either a fast Fermi chopper or a rotating crystal rather resembling the double rotating crystal spectrometer IN4 at ILL. At its first meeting the Science Planning Group (SPG) of the SNS selected 11 instrument types which were deemed to be "of primary interest". The 'Moderate' Energy Transfer Spectrometer was included in this group.

Subsequently it was decided that, while five instruments were ready to proceed to the design stage, the Medium Energy Transfer Spectrometer (MET) required firmer technical specification particularly with respect to the method of monochromating the incident beam. A working group within the Neutron Division was set up to examine the design of the spectrometer. It was recognised that a long (~ 4m) secondary flight path was required. Furthermore in order to maximise the coverage of momentum transfers this dictated that a vertical scattering plane was necessary, with the large detector bank being housed in a hole beneath the floor of the experimental hall. A beam hole viewing the 95K methane moderator was identified (S6), and during excavations for the foundations of the neutrino bunker the necessary civil engineering work to provide the hole for the large detector bank was completed. At that time a more restricted financial ceiling was imposed on the SNS project as a whole and further capital spend on MET was put into abeyance.

In the meantime two development programmes, which are pertinent to the design of this spectrometer, were underway. An inelastic spectrometer using a Fermi chopper monochromator was installed on the newly commissioned Harwell electron linac pulsed source. The Inelastic Rotor Spectrometer [4] was part of the UKAEA/SERC joint neutron scattering programme and was designed as a prototype for the SNS High Energy Transfer Spectrometer, HET. In practice, because of its range of incident energies and the wide range of scattering angles the spectrometer also gave valuable experience in the area of interest to the medium energy transfer spectrometer. The second development programme of relevance encompassed the use of crystal monochromators on pulsed sources. Stationary crystals can offer advantages over rotating choppers which require precise phasing to a source which itself is not absolutely periodic. These studies were both theoretical [5,6] and experimental [7] and involved a collaboration with the PTB Braunschweig. Neutron measurements were carried out at the PTB reactor and the Harwell linac.

Other designs have been proposed for the Medium Energy Transfer Spectrometer over the past seven years; these include the use of correlation choppers [8] and of pulsed ferrite monochromators [9]. Although these are interesting and novel suggestions, they cannot readily

be incorporated into designs which are consistent with the required instrument specification.

The main activity on MET during the last year has been an examination of the use of crystal and choppers as the incident beam monochromator. A preliminary paper has been published [10]; it concludes by recommending that a hybrid spectrometer should be built with conventional fast Fermi choppers for high incident energies, and a double crystal arrangement for low energies. In this report we give a more complete account of the comparison between crystal and chopper spectrometers, and discuss some of the practicalities of implementing the recommendations of reference [10].

2. SCIENTIFIC APPLICATIONS

In this section we briefly review the scientific applications of the spectrometer and refer to the instrument design parameters needed to perform the experiments. There are four main categories:

2.1 Coherent Excitations

A major part of the research program on this instrument is expected to involve the measurement of the dynamic structure factors $S(Q,\varepsilon)$ in polycrystalline and amorphous solids, liquids and gases. It is necessary to take data over a large range in Q and with incident energies up to ~ 500 meV. The incident energy resolution needed is $\Delta E_1/E_1 \sim 1\%$ and the Q resolution $\Delta Q/Q \sim 2\text{-}3\%$.

2.2 Magnetism

It has become evident in recent years that in order to explain the magnetic properties of 3d-systems there is a need to measure the magnetic response over the whole excitation spectrum, and to place this on an absolute scale. Strong exchange effects produce steep spin waves which merge into a broad particle-hole continuum. It is therefore necessary to follow the magnetic excitations to as high an energy transfer as possible while maintaining low values of Q (say $Q < 4\text{Å}^{-1}$) due to the fall-off of the magnetic form factor. Although the magnetic response is concentrated in the low angle detectors, it is essential to take data over a very wide scattering angle range in

order to take proper account of the phonon scattering. For such measurements the required incident energy should approach 1 eV and the energy and wavevector transfer resolutions $\Delta\varepsilon/\varepsilon \sim \Delta Q/Q \sim 1\text{-}2\%$.

Another class of magnetic measurement for which this spectrometer is suited is magnetic spectroscopy in f-electron metals and alloys. Stable moments can give sharp line spectra from which crystal field and spin-orbit splittings (ranging from 10^{-4} to $\sim$ 1 eV) can be deduced. Good energy transfer resolutions, $\Delta\varepsilon/\varepsilon \sim 1\text{-}2\%$, are required, though the Q-resolution (at $Q < 4\text{Å}^{-1}$) can be much more relaxed ($\Delta Q/Q \sim 10\%$). In cases where the moments become unstable due to some hybridisation of f and conduction electrons, e.g. as in mixed valence materials, the spectra can become broad and lower resolutions in $\Delta\varepsilon/\varepsilon$ may be tolerated.

2.3 Molecular Spectroscopy

The energy transfer resolutions required in this field of study are at their most severe since they compare unfavourably with optical techniques. There remain however many materials which cannot readily be studied optically e.g. metal-hydrogen systems, samples in complicated environments, or catalysers on substrates, where neutron spectroscopy from hydrogen is a powerful method. It is essential to have the capabilities of measuring a whole range of energy transfers ($\sim$ 10 to $\sim$ 200 meV) at the highest possible energy resolution ($\Delta\varepsilon/\varepsilon \sim 1\%$ is consistent with useful intensities) and at both large and small scattering vectors Q. In general the Q resolution can be very relaxed ($\Delta Q/Q \sim 10\%$), but there are instances where it is desirable to follow the weak dispersion of a mode with Q and here $\Delta Q/Q \sim 2\text{-}3\%$ is more appropriate. In addition, assignments in complex molecules or potential model fitting in simple systems both benefit by studying peak intensities as a function of temperature and Q. The good Q-resolution of the spectrometer is an attractive feature for such measurements.

2.4 Momentum Distributions

The advent of pulsed sources during recent years has created an upsurge in the use of high energy neutrons to measure momentum

distributions [11,12]. In order to limit ambiguities the essential requirement is to measure the dynamic scattering factor $S(Q,\varepsilon)$ at large Q's where the impulse approximation becomes valid. In this regime the dynamic response is given by the recoil energy $E_r = Q^2/2M$, but additionally (and as a further check of the data) the width of the peak at constant Q is proportional to Q. The proposed spectrometer, when used with high incident energy neutrons, can make important contributions to this field since it allows large and suitably high regions of Q to be accessed at high resolution; for the measurements it is therefore essential to provide a closely-packed set of high angle detectors. An impressive set of results from various helium systems has already been obtained on the IPNS chopper spectrometers [13,14].

3. CURRENT SPECIFICATION

3.1 Dynamic Range and Resolution

In order to carry out the scientific programmes outlined in Section 2 we require the following spectrometer characteristics: (a) energy transfers ε up to approximately 1 eV should be measurable over (b) as wide a possible scattering vector Q range, with (c) resolutions approaching 1% in both $\Delta\varepsilon/\varepsilon$ and $\Delta Q/Q$. The wide range in Q can only be achieved in a direct geometry instrument, and for this we require incident energies E_1 up to ~ 1 eV, with $\Delta E_1/E_1$ better than 1% in order to fulfill the resolution requirements. The wide dynamic range is achieved by providing an effectively continuous number of incident energies E_1, and a very large detector bank where the scattering angle limits are determined by incident beam contamination effects at forward angles and structural considerations at backward angles.

Thus the current specification calls for a range of incident energies from ~ 20 meV to 500 meV or greater, with a continuous range of scattering angles from 5° to 135°. Low Q experiments will be facilitated by providing a circularly symmetric detector over the angular range 5°-10°. Part of this detector will be supplied with finer angular resolution detector elements; this is important for single crystal excitation experiments. The dynamic range accessible with such a spectrometer is shown in Figure 1.

3.2 Comparison with existing spectrometers

The most intense equivalent reactor-based spectrometer presently operating is IN4 at ILL. It has an energy transfer resolution of between 2 and 4% for energy transfers up to 80 meV. Whilst maintaining an equivalent monochromatic flux at the sample, this spectrometer will exceed the capabilities of IN4 both in energy transfer range and resolution.

The two chopper spectrometers LRMECS and HRMECS in operation at the Argonne IPNS are arguably the best inelastic spectrometers currently available on a pulsed source [15]. This spectrometer will achieve the same dynamic range as these instruments but at higher energy transfer resolution; the intensity at the sample position is also predicted to be higher at full SNS current.

4. RESOLUTIONS

We shall restrict our discussion to two monochromating devices, namely Bragg scattering from a single crystal or velocity selection by a mechanical chopper phased to the pulsed source. These determine the incident energy, with some associated uncertainty, and time-of-flight to the detector, with an associated uncertainty, is used to determine the scattered neutron energy. A description of the important parameters which determine the resolution is aided by reference to the distance-time diagrams shown in Figure 2. The moderator, chopper, scattering sample and detector are denoted by M, CH, S and D respectively. E_1 and E_2 represent the incident and final neutron energy and the energy transfer, ε, is given by

$$\varepsilon = E_1 - E_2 \qquad (1)$$

For both spectrometers the measurable parameter is the time-of-flight to the detector, t_D. An effective energy transfer is obtained by assuming a well-defined incident energy thus allowing the final flight time, and hence the final energy, to be determined. In order to determine the error in ε we associate the timing error at the detector Δt_D with an energy uncertainty in E_2 (and hence ε) :

$$\Delta\varepsilon = \frac{\partial\varepsilon}{\partial t}\Delta t = 2\frac{E_2}{t_2}\Delta t_D \qquad (2)$$

This is equivalent to identifying the observed time uncertainty at the detector, Δt_D, as an energy uncertainty in E_2 which has been propagated, by dispersion from a unique E_1, over the secondary flight path of the spectrometer.

4.1 Crystal Monochromator Energy Transfer Resolution

For the crystal spectrometer the monochromator acts as a wavelength selector with resolution

$$R' = \Delta\lambda/\lambda = \cot\theta.\Delta\theta = \Delta t'/t \qquad (3)$$

A purely dispersive time width $\Delta t'_s$ at the sample due to this resolution is propagated, after inelastic scattering, to an observed width at the detector

$$\Delta t'_D = \Delta t'_s \left[1 + \frac{L_2}{L_1}\left(\frac{E_1}{E_2}\right)^{3/2}\right] \qquad (4)$$

(Primes are used to denote time widths (FWHM) which are related to velocity uncertainties and double primes indicate pure timing errors).

Interpreting this width as an uncertainty in ε, from equation (2):

$$\frac{\Delta\varepsilon'}{E_1} = 2R'\left[1 + \frac{L_1}{L_2}\left(1 - \frac{\varepsilon}{E_1}\right)^{3/2}\right] \qquad (5)$$

where $R' = \Delta t'_1/t_1$ is the resolution of the monochromator. Non-dispersive time uncertainties, such as the moderator pulse width, contribute a term, from equation (2):

$$\frac{\Delta\varepsilon''}{E_1} = 2R''\left[1 - \frac{\varepsilon}{E_1}\right] \qquad (6)$$

where $R'' = \Delta t''_M/t_2 = \delta_m/L_2$ and δ_m is (for the SNS) the 28 mm positional uncertainty associated with the moderator in the slowing down part of

the spectrum. The overall resolution of the crystal spectrometer is then the sum in quadrature of equations (5) and (6):

$$\frac{\Delta\varepsilon}{E_1} = \left[\{2R'\left[1 + \frac{L_1}{L_2}\left(1 - \frac{\varepsilon}{E_1}\right)^{3/2}\right]\}^2 + \{2R''\left[1 - \frac{\varepsilon}{E_1}\right]\}^2\right]^{\frac{1}{2}} \qquad (7)$$

4.2 Phased Chopper Energy Transfer Resolution

A similar expression may be derived for the case of a chopper spectrometer. The contribution to the velocity selection from the chopper open time Δt_{CH} gives, in an analagous way to the crystal:

$$\frac{\Delta\varepsilon'}{E_1} = 2R_1'\left[1 + \frac{d_1 + d_3}{d_2}\left(1 - \frac{\varepsilon}{E_1}\right)^{3/2}\right] \qquad (8)$$

with $R_1' = \Delta t_{CH}/t_{CH}$. Here Δt_{CH} is a convolution of the intrinsic burst time defined by the slit package and a scan time across the moderator face. For the geometries under consideration, the scan time is only important for energies greater than 400 meV. Even then, its contributions may be minimised by the use of a suitably angled moderator [4].

The chopper resolution has an additional dispersive component due to the moderator pulse width:

$$\frac{\Delta\varepsilon'}{E_1} = 2R_2'\left[1 + \frac{d_3}{d_2}\left(1 - \frac{\varepsilon}{E_1}\right)^{3/2}\right] \qquad (9)$$

with $R_2' = \Delta t_M'/t_{CH} = \delta_m/d_1$

The overall energy transfer resolution of a chopper device is then the sum in quadrature of the two dispersive terms:

$$\frac{\Delta\varepsilon}{E_1} = \left[\{2R_1'\left[1 + \frac{d_1 + d_3}{d_2}\left(1 - \frac{\varepsilon}{E_1}\right)^{3/2}\right]\}^2 + \{2R_2'\left[1 + \frac{d_3}{d_2}\left(1 - \frac{\varepsilon}{E_1}\right)^{3/2}\right]\}^2\right]^{\frac{1}{2}}$$

(10)

Typical calculations of time widths and energy resolutions using this model have been compared with results using a RAL Monte Carlo code which simulates the behaviour of a chopper spectrometer on a pulsed source; the agreement between the two methods was shown to be good.

4.3 Discussion

The functional dependence of the dimensionless resolution $\Delta\varepsilon/E_1$ on the fractional energy transfer ε/E_1 is clearly different in the two spectrometers, so that it is not immediately obvious what value of ε/E_1 we should be taken in comparing performances. As an example, we calculate the resolution of a chopper spectrometer with d_1 = 9m, d_3 = 1m and d_2 = 4m and with Δt_M matched to Δt_{CH} and compare this to a L_1 = 7m, L_2 = 4m crystal spectrometer with R' chosen to match the chopper's resolution at ε = 0. These calculations are illustrated in Figure 3. From this figure we note that the overall behaviour of the two functions is sufficiently similar that we may choose to match at other values of ε/E_1 without introducing a significant bias. In the ε = 0 limit, the resolution of both spectrometers is the convolution of R' or R'' terms, with the R' terms amplified by geometric factors. The $\varepsilon = E_1$ limit differs in the two cases. For the chopper it is a convolution of two R' terms, but in the crystal case it simply contains one R' term, that due to the resolution of the monochromator itself. Figure 3 also illustrates the fractional energy transfer required to provide a given fractional energy resolution $\Delta\varepsilon/\varepsilon$. The area of Q-$\varepsilon$ space accessible at a given resolution is significantly less than that given by the kinematic condition:

$$\frac{\hbar^2 Q^2}{2m} = E_1 + E_2 - 2\sqrt{E_1 E_2}\cos\phi \qquad (11)$$

where ϕ is the scattering angle.

Figure 4 shows contours of Q-ε space accessible for a set of resolutions in the case of a direct geometry instrument with infinitely variable E_1. A reasonable 'rule of thumb' which balances Q-ε range and resolution is the condition:

$$\frac{1}{3} < \frac{\varepsilon}{E_1} < \frac{2}{3} \qquad (12)$$

The resolution expressions derived in the preceding sections also have important implications in the optimisation of the instrument geometries. In the crystal spectrometer R' and R'' do not depend on L_1, and for intensity reasons a short L_1 is preferable. In the chopper spectrometer both R_1' and R_2' are inversely proportional to d_1 which implies that large values of the primary flight path are required for high resolution. In discussing the geometric optimisation of the chopper spectrometer it is convenient to express equation (10) for matched chopper and moderator pulse widths ($R_1'=R_2'=R$) and for elastic scattering $\varepsilon=0$:

$$\frac{\Delta\varepsilon}{E_1} = 2R.\frac{1}{d_2}\{(d_1 + d_2 + d_3)^2 + (d_2 + d_3)^2\}^{\frac{1}{2}}$$

$$\alpha\ G(d_1,d_2,d_3) = \frac{1}{d_1 d_2}\{(d_1 + d_2 + d_3)^2 + (d_2 + d_3)^2\}^{\frac{1}{2}}. \qquad (13)$$

The behaviour of this equation and its relevance to the chopper spectrometer design are described in Section 5.

4.4 Scattering Vector Resolution

The main contributions to the scattering vector resolution ΔQ come again from Δt_D, (see equation (2)) together with a term due the uncertainty in the scattering angle ϕ. For the crystal spectrometer and isotropic beam divergences we find:

$$\Delta Q = \frac{2m\sqrt{E_2}}{\hbar^2 Q}\left\{\frac{2E_2}{mL_2}\left[E_1^{\frac{1}{2}}\cos\phi - E_2^{\frac{1}{2}}\right]^2 \Delta t_D^2 + E_1\sin^2\phi.\Delta\phi^2\right\}^{\frac{1}{2}} \qquad (14)$$

with d_2 replacing L_2 for the chopper spectrometer. This may be written in terms of the energy transfer resolution $\Delta\varepsilon$ as

$$\Delta Q = \frac{2m}{\hbar^2 Q}\left\{\frac{1}{4E_2}\left(E_1^{\frac{1}{2}}\cos\phi - E_2^{\frac{1}{2}}\right)^2 \Delta\varepsilon^2 + E_1E_2\sin^2\phi.\Delta\phi^2\right\}^{\frac{1}{2}} \qquad (15)$$

The behaviour of ΔQ as a function of the incident energy E_1 with energy transfer resolution $\Delta\varepsilon/\varepsilon = 0.01$ is shown in Figure 5 for different scattering angle uncertainties $\Delta\phi$ where $\phi = 20°$. We note

that for fixed $\Delta\varepsilon/\varepsilon$, or equivalently fixed E_2/E_1, $\Delta Q/Q$ depends simply on ϕ and $\Delta\phi$, and this is illustrated in Figure 6 for the $\Delta\varepsilon/\varepsilon = 0.01$ case. We infer that, even in this good $\Delta\varepsilon$ resolution example, the scattering vector resolution at low ϕ is dominated by timing errors rather than by $\Delta\phi$. For example at $\phi = 20°$ the matching angular term requires a relatively large divergence $\Delta\phi \sim 1.5°$ but still gives a reasonable $\Delta Q/Q \sim 1.7\%$. The Q resolution improves at higher scattering angles and here the contribution from the divergence term becomes increasingly more important; see particularly at $\phi \sim 60°$.

We emphasise that Figure 6 pertains only for the $\Delta\varepsilon/\varepsilon = 0.01$ case. The zero minimum in the $\Delta Q/Q$ curve for $\Delta\phi = 0$ is simply given by equating $E_1^{\frac{1}{2}}\cos\phi$ and $E_2^{\frac{1}{2}}$ (i.e. $k_1\cos\phi = k_2$) in equations (14) and (15), and therefore depends critically on E_2/E_1 and the energy transfer resolution $\Delta\varepsilon/\varepsilon$. For small energy transfers ($E_2 \sim E_1$) we observe from equation (15) that at small ϕ the $\Delta\phi$ contribution to the scattering vector resolution dominates, since the second term in this equation approaches zero.

5. INTENSITIES

Apart from practicality considerations, the single most important parameter which determines the effectiveness of a monochromating device is the intensity it produces at the sample position for a fixed energy resolution. In evaluating the chopper and crystal methods we consider the spectrometer to view the 95K SNS liquid methane moderator. Since the secondary spectrometers (i.e. flight paths and solid angles) are assumed to be identical the comparison entails calculating the intensities at the scattering sample positions for the same energy transfer resolution which we set at 1% for $\varepsilon = E_1$ i.e. $\Delta E_1/E_1 = 0.01$. The intensity at the sample is given by:

$$I(E_1) = \frac{6 \times 10^{12}}{L^2} \frac{\Delta E_1}{E_1} T(E_1) \qquad (16)$$

where $L \equiv L_1 \equiv d_1 + d_3$ and $T(E_1)$ is the transmission efficiency of the monochromating device. We now estimate these intensities for various crystal monochromator arrangements and a fast Fermi chopper as a function of the incident neutron energy E_1.

5.1 Crystal Spectrometer

We begin with the premise that the instrument has a fixed take-off angle (2θ), this being largely dictated by the difficulty in rotating a large heavily-shielded detector. At fixed resolution this immediately determines the acceptable beam divergence at the monochromator since $(\Delta E_1/E_1) = 2\cot\theta.\Delta\theta$. This relation imposes appreciable intensity penalties at high incident energies where both θ and $\Delta\theta$ are small, and this under-illumination problem is the principal reason why crystals are uncompetitive with choppers at high energies. The situation is however alleviated considerably at lower energies since it is then possible to operate at relatively large Bragg angles.

The illumination criterion is illustrated in Figure 7, where Curve A is the universal 1% constant resolution relation shown as a function of corresponding pairs of take-off angle 2θ and FWHM Bragg angle width $\Delta\theta$. In a symmetrically collimated arrangement $\Delta\theta$ is equal to $\sqrt{2}\alpha$, where α is the beam divergence before and after the monochromator. Good illumination occurs when the natural available collimation in the incident beam is equal to or greater than $\Delta\theta/\sqrt{2}$, where $\Delta\theta$ is dictated by resolution requirements. We also show the moderator-crystal monochromator distance L(m) at which illumination matching occurs for the 10 cm wide SNS moderators, together with the $\Delta\theta$ values.

In the crystal spectrometer under discussion both resolution and intensity arguments demand that L should be as short as possible, but practical considerations suggest L ~ 7m to be close to the optimum. The consequences of this on the crystal illumination are that regions above Line B in Figure 7 are well-illuminated, whereas those below are badly illuminated. A further consequence, which becomes evident on examining the Bragg condition with a typical d-spacing d = 1.08Å for monochromatisation at energies E_1 (Curve C), is that the well-illuminated region occurs at large take-off angles and low energies E_1. Further detailed modifications to Curves A and C can be effected by changing the required resolution or crystal d-spacing respectively, however the general argument persists, and we conclude that adequate illumination in the crystal spectrometer is only possible at large take-off angles and with low incident energies.

In calculating intensities it is more convenient to express equation (16) in terms of the integrated crystal reflectivity $R(\theta)$, which is effectively the angular range over which the crystal may be considered to have unit reflectivity. $R(\theta)$ is related to the equivalent energy width $R(E_1)$ by the differential of the Bragg condition in terms of energy ($E^{-\frac{1}{2}} \propto \sin\theta$):

$$\begin{aligned} R(E_1) &= 2E_1 \cot\theta . R(\theta) \\ &= T(E_1) . \Delta E_1 \end{aligned} \tag{17}$$

and substitution into equation (16) gives

$$I(E_1) = \frac{6 \times 10^{12}}{L_1^2} . 2\cot\theta . R(\theta) \tag{18}$$

In the calculations to be presented, $R(\theta)$ were determined using the transmission geometry formalism of Popovici and Gelberg [16] which includes secondary extinction. These theoretical values are however rarely achieved in practice due to the presence of simultaneous reflections and deviations of the microstructure of a real crystal from the ideally imperfect definition assumed in the theory. We therefore include a factor of T' in the intensity expression to take this into account:

$$I(E_1) = \frac{6 \times 10^{12}}{L_1^2} . 2R(\theta) \cot\theta . T' \tag{19}$$

The equation is valid for 'open' or natural collimation geometries. Intensity estimates have been made for copper and pyroltic graphite monochromator crystals. For the former we have used a loss factor $T' = 0.8$, which has been justified by experimental data [7]. For pyrolytic graphite it is widely accepted that these losses are small and we have assumed $T' = 1$. The Cu calculations were performed for a room temperature crystal with $L_1 = 10m$, 1% incident energy resolution, and $2\theta \simeq 90°$. These intensities are shown in Figure 8A, though it must be emphasised that this performance cannot be achieved continuously over the whole range, as the calculation is based on optimised crystal thicknesses and mosaics at selected energies

corresponding to available d-spacings. These values can be readily enhanced by i) a factor x 2 by using reflection rather than transmission geometry and ii) a further factor x 2.5 by using a number of monochromators in an 'out-of-plane' focussing array [17]; the estimated intensities are then given by Figure 8B. Pyrolytic graphite (PG) is a more efficient monochromator than Cu in the thermal and cold neutron region and we show estimates of the intensities for a single PG monochromator in Figure 8C; these were calculated using the method of Riste and Otnes [18]. Finally we have considered the implications of using a double PG crystal array in an out-of-plane focussing geometry and show the calculated intensities in Figure 8D. We believe that these intensities should be achievable in practice, and this arrangement provides the facility of allowing the incident energy to be changed continuously.

5.2 Chopper Spectrometer

In order to make a direct comparison with the crystal spectrometer intensity calculations at fixed incident energy resolution $\Delta E_1/E_1 = 0.01$ it is first necessary to determine the instrument geometry i.e. the source-chopper distance d_1 that gives, for matched moderator and chopper open times (or $R_1' = R_2'$), a resolution 2 R_{CH}' of 1%. A solution of equations:

$$R_{CH}' = [(R_1')^2 + (R_2')^2]^{\frac{1}{2}} = 0.005 \tag{20}$$

and

$$R_2' = \frac{\delta m}{d_1} = \frac{1}{36 d_1} \tag{21}$$

determines the geometry $d_1 = 7.86$m, $d_3 = 1$m, $d_2 = 4$m. The intensity on the sample, equation (16), is in this case:

$$I_{CH}(E_1) = \frac{6 \times 10^{12}}{(d_1 + d_3)^2} \; 2R_{CH}' T(E_1) \tag{22}$$

$$= 5.4 \times 10^4 \; T(E_1) \; n/cm^2/s \tag{23}$$

where $T(E_1)$ is the chopper transmission. For a Fermi chopper slit package this depends on several factors which include geometrical

attenuation, collimation, shadowing and imperfections in manufacture. These have been discussed in [6] and estimated to be:

$$T(E_1) = 0.72 - 0.6E_1 \qquad (24)$$

where E_1 is expressed in eV.

The resultant intensities calculated at the sample position over the slowing down region are shown in Figure 8E. It should be noted that this continuous behaviour is again not achievable in practice for the chopper spectrometer, since only a finite number of slit packages each optimised to a given E_1, can be made.

In deciding the optimum practical moderator-chopper distance in the spectrometer we set a premise that an energy transfer resolution $\Delta\varepsilon/\varepsilon = 0.01$ should be achievable over a large range of Q-ε space. This is only possible if $\Delta E_1/E_1$ is reduced below 0.01, which at matched moderator and chopper time widths necessitates increasing d_1 i.e. $d_1 \gtrsim 7.86$m. One obvious disadvantage of increasing d_1 is that this is only possible at the expense of intensity which falls approximately as d_1^3. For this spectrometer we recommend $d_1 = 10$m since i) this allows a primary flight path which is close to the minimum which may be built due to the spatial constraints imposed by a wide angle detector bank on the layout, and ii) the energy transfer specification is fulfilled - $R'_{CH} = 0.00393$ or $\Delta E_1/E_1 = 0.00786$ for matched time widths.

We now examine the d_2-dependence of the energy transfer resolution term $\Delta\varepsilon/E_1$. Following equation (13) this is plotted in Figure 9 for $d_1 = 10$m and $d_3 = 1$m, with matched resolutions $R = \delta_m/d_1 = 0.0028$, where δ_m is the 28mm positional uncertainty for the moderator in the slowing down region of the spectrum. The figure shows that though large gains in resolution result as d_2 is increased, the geometric factor G quickly saturates, and only marginal improvements ensue for $d_2 \gtrsim 4$m. A scattered flight path of 4m also allows a major part of the available solid angle to be filled with detectors.

Other criteria such as mismatching the chopper and moderator time structure may be desirable in some circumstances, for example at very

high incident energies, but they are not appropriate in the design optimisation of this spectrometer. The recommended configuration is therefore a chopper at 10m from the source with the sample as close to this as collimation allows, with a complete detector bank at 4m from the scattering sample.

5.3 Summary

The general conclusion from Figure 8 is that the chopper spectrometer provides greater intensities towards large neutron energies, but that crystal monochromators can perform better towards lower energies. The cross-over energies are approximately 100 meV for an out-of-plane focussed Cu crystal array and 40 meV for a double PG monochromator system. It should be noted that these curves are only appropriate for the fixed incident energy resolution $\Delta E_1/E_1 = 0.01$, and that the cross-over shifts towards lower E_1 values as this resolution is improved. For the spectrometer under discussion, where in practice we require $\Delta E_1/E \sim 0.008$, the shifts in the cross-over energies will be minimal and do not affect this general conclusion.

6. PRACTICALITIES

6.1 Number of Incident Neutron Energies

In a direct geometry spectrometer with a large angular array detector the main limitation to the (Q,ε) range which can be accessed is determined by the number of incident energy (E_1) settings available. In the case of the chopper spectrometer this is only a relatively minor restriction, since a set of rotors can, in principle, be phased with the source to provide a continously variable E_1. For a fixed take-off angle crystal spectrometer a given combination of crystals or crystal planes can only provide a finite number of E_1 values.

Equation (12) provides a first indication of the number of E_1 values required to give reasonable resolution and (Q,ε) space coverage. If the maximum incident energy needed is E_M, then this condition can be met by producing other monochromatic beams with energies $E_M/2$, $E_M/4$, $E_M/8$, etc. This criterion can be satisfied by both types of spectrometer, and provides broad (Q,ε) range coverage with fractional energy transfer resolutions better than approximately 5% (see Figure 3).

The current trends in the scientific applications outlined in Section 2 are now directed towards the measurement of absolute cross-sections and line shapes, and in order to minimise corrections to measured data it is widely accepted that resolutions ~ 1% are now needed even for broad scattering distributions. Figures 3 and 4 show that this can only be achieved at the expense of (Q,ε) range, and also that fractional energy losses $\varepsilon/E_1 \sim 0.90$ are necessary. One consequence of this is that it requires the incident energies E_1 to be continuously changeable in steps ~ 10%; this is in principle achievable up to incident energies $E_1 \sim 1$ eV only in the case of the chopper spectrometer. Continuous changes in E_1 are also possible with a double monochromator system, and we have shown that they give high intensities at low energies.

6.2 Crystal Spectrometer

An important practical issue for the crystal spectrometer is that the monochromator produces, in addition to a beam of wavelength λ, order contamination at $\lambda/2$, $\lambda/3$, ... etc. This has the possible advantage of simultaneously producing several utilisable incident energies, but has the disadvantage that inelastic spectra from the different orders may overlap. The effects of higher order reflections on the time-of-flight spectra of crystal spectrometers has been analysed in detail in reference [10]. It was concluded that on balance these are undesirable, since it is unlikely that they will produce good quality data and may cause unwanted backgrounds.

Crystal spectrometers do have several advantages, the most notable being a) they allow the sample to be placed out of the main incident beam which gives lower backgrounds, b) the instrument can be designed to have no moving parts, c) there is some scope for improving intensities particularly be using focussing techniques [17], and d) the monochromators require very little maintenance. There are however two overwhelming arguments why a fixed crystal arrangement is not a suitable choice for the spectrometer under discussion: the first is that it gives progressively lower and uncompetitive intensities as E_1 increases, and secondly it can only provide a very restricted number of incident energies. It has already been mentioned that these deficiencies do not apply at lower energies where a double crystal arrangement becomes a feasible option.

6.3 Chopper Spectrometer

The main disadvantages of choppers are that they are mechanically and electronically complex since they must be phased precisely with the pulsed source and they often require a considerable amount of maintenance. The most satisfactory solution to the phasing problem is to run both the chopper and the accelerator from a crystal clock and this is what is proposed at the SNS. We also recommend using a magnetic bearing drive system as used on the SNS HET spectrometer [19]. Despite these complexities the chopper monochromator is uniquely suited for this spectrometer since it is the only method which, when equipped with a suitable suite of rotor packages, can provide continuously variable incident energies up to ~ 1 eV with adequate transmission and resolution. The chopper method is also a well-established technique on pulsed sources [15] and is the obvious choice as the main monochromator for this instrument.

7. RECOMMENDED DESIGN

The recommended design, based on the arguments of this paper is illustrated in Figure 10. Initially the instrument would be a conventional chopper, but the design allows the addition of a double monochromator system at a later stage as the SNS current increases and the source becomes more competitive at lower energy transfers.

7.1 Moderator Choice

The optimum moderator choice for this spectrometer is the 95K gadolinium poisoned methane moderator. This provides an intense slowing down spectrum until 50 meV and good intensity down to 20 meV without significant degradation of resolution [19]. An appropriate beamline, S6, which views the methane moderator at 13° to the normal, has been reserved for this spectrometer.

7.2 Chopper

Space constraints imposed by neighbouring instruments force this spectrometer to operate in the vertical plane, despite the increased complexity of the sample environment. It is possible to relax the

collimation in the out-of-plane dimension thus giving a rectangular beam at the sample of typically 8 cm wide x 5 cm high. To produce such a beam it is desirable to spin the chopper about a horizontal axis. This is feasible with the magnetic bearing system. Chopper frequencies up to 600 Hz will be required to produce a burst width matched to the moderator pulse over the entire energy range. It may be possible to reduce the number of different choppers required by rephasing and operating at different multiples of the SNS frequency. Such a scheme will be investigated on HET.

A second chopper, closer to the source, may be desirable to reduce background. The favoured concept is a high speed nimonic chopper, similar to the monochromating device, but with say 10 times the burst width. The two choppers would be phased together and both would be closed after the burst to suppress background during the times corresponding to the arrival of downscattered neutrons at the detector. A 10 cm diameter nimonic device is equivalent to 16 mean free paths at energies below 1 eV, an attenuation of 1 in 10^7. A much larger object would be required to provide this attenuation for fast neutrons, but such neutrons, even if moderated in the spectrometer shielding, should be easily discriminated by their time of arrival.

7.3 Hybrid Concept

The section of collimator and shielding between the coarse chopper and the monochromating chopper will be designed to be removable, thus allowing the later addition of a primary beam polarising filter, other in-beam devices such as further background suppressing choppers or filters, or the implementation of the hybrid spectrometer concept.

The double monochromator concept discussed in reference [10] operated in the vertical plane. This required a realignment of the entire secondary spectrometer and led to some difficulties with beam stop design. A preferable approach is to use the double monochromator to displace the beam horizontally say 30 cm to a second sample position. Parallax errors between sample and detector at all but the smallest angles are unimportant and the low angle problem would be resolved by using a rectangular grid detector and mapping onto the appropriate rings in software. Even without the hybrid option this is the preferable design for the low angle array.

7.4 Detectors

A major part of the cost of this instrument is its detector system. Scintillator detectors will be used in standard double photomultiplier tube modules of say 10 x 4 cm^2. Three modules will be added to give a detector 30 cm in the out of plane dimension but with 0.6° in-plane resolution which is suitable for single crystal work. At low angles a rectilinear array of single photomultiplier tube 5 x 5 cm^2 modules will be used.

8. CONCLUSIONS

We are led to the conclusion that two different monochromating devices are required ideally to provide incident energies in the range from 20 meV up to about 1 eV. An out-of-plane focussed, pyrolytic graphite double monochromator is the obvious choice at low energies, say $E_1 < 40$ meV, and a phased mechanical chopper is favoured at all higher energies. The secondary spectrometer is however a large and very expensive array of detectors covering the maximum solid angle and only one can be built on SNS. We therefore propose that such a secondary spectrometer is shared between the two monochromating devices on the one beam hole. This scheme is illustrated in Figure 10.

It is now evident that the unique feature of the proposed spectrometer is not its medium incident energy or energy transfer range (indeed we are now proposing its use up to 1 eV incident energies), but rather its large and closely spaced detector array. We therefore suggest that it should henceforth be called a Multi-Angle Rotor Spectrometer - MARS; this name also conveniently denotes that it has the rotor as its primary monochromator.

REFERENCES

[1] A.D. Taylor, 'A medium energy inelastic spectrometer for SNS' Rutherford Appleton Laboratory Report NDR/P11/83 (1983).

[2] B.E.F. Fender, L.C.W. Hobbis and G. Manning, Phil. Trans. Roy. Soc. Lond. B90 657 (1980).

[3] L.C.W. Hobbis, G.C. Stirling, and G.H. Rees, 'A pulsed neutron facility for condensed matter research' Rutherford Appleton Laboratory Report RL 77/064C (1977).

[4] B.C. Boland, D.F.R. Mildner, G.C. Stirling, L.J. Bunce, R.N. Sinclair and C.G. Windsor, Nucl. Instrum. and Meth. 154 349 (1978).

[5] C.J. Carlile and W.G. Williams, 'Inelastic neutron scattering using a crystal spectrometer on a pulsed source' Rutherford Appleton Laboratory Report RL-81-028 (1981).

[6] C.J. Carlile and W.G. Williams, 'A comparison of crystal and chopper spectrometers on the SNS' Rutherford Appleton Laboratory Internal Report NDR/P6/83 (1983).

[7] C.J. Carlile, W.G. Williams and V. Wagner, 'Inelastic neutron scattering using a crystal spectrometer on a pulsed source: Experimental tests of copper monochromators' Physikalisch-Technische Bundesanstalt Report FMRB-104 (1984).

[8] L. Cser, 'Correlation spectroscopy on a pulsed source' Rutherford Appleton Laboratory Internal Report, unpublished.

[9] R. Cywinski, 'Magnetically switched ferrite monochromators on pulsed neutron sources' Rutherford Appleton Laboratory Report NDR/P1/83 (1983).

[10] C.J. Carlile, A.D. Taylor and W.G. Williams, Proc. IAEA Conf. 'Neutron scattering in the nineties' Jülich 1985, IAEA-CN-46/008P.

[11] R.O. Simmons, Proc. 1984 Workshop on High Energy Excitations in Condensed Matter, Los Alamos National Laboratory Report LA-10227-C, Vol. II 416 (1984).

[12] A.D. Taylor, ibid. 512 (1984).

[13] R.O. Hilleke, P. Chaddah, R.O. Simmons, D.L. Price and S.K. Sinha, Phys. Rev. Lett. 52 847 (1984).

[14] P.E. Sokol, K. Sköld, D.L. Price and R. Kleb, Phys. Rev. Lett. 54 909 (1985).

[15] D.L. Price, J.M. Carpenter, C.A. Pelizzari, S.K. Sinha, I. Bresof, and G.E. Ostrowski, Proc Sixth Int Collab on Advanced Neutron Sources, Argonne National Laboratory Report ANL-82-80, 208 (1982).

[16] M. Popovici and D. Gelberg, Nucl Instr and Meth 40 77 (1966).

[17] R. Scherm and V. Wagner, Neutron Inelastic Scattering IAEA Vienna (1978) 149.

[18] T. Riste and K. Otnes, Nucl Instr and Meth 75 197 (1969).

[19] A D Taylor, 'SNS Moderator Performance Predictions' Rutherford Appleton Laboratory Report RAL-84-120 (1984).

FIGURE CAPTIONS

Figure 1: The kinematic space, in dimensionless units, covered by a direct geometry spectrometer with a scattering angle range $5° < \phi < 135°$.

Figure 2: Distance - Time diagrams for a crystal monochromator spectrometer and a phased chopper spectrometer on a pulsed neutron source.

Figure 3: The resolution in energy transfer versus energy transfer in reduced units for a crystal and a chopper monochromator matched at $\varepsilon = 0$. Fractional energy transfer resolutions are also indicated.

Figure 4: The variation in fractional energy transfer resolution over Q-ε space.

Figure 5: Scattering vector resolution as a function of the incident energy for an energy transfer resolution $\Delta\varepsilon/\varepsilon = 0.01$ at $\phi = 20°$ with various $\Delta\phi$.

Figure 6: Fractional scattering vector resolution as a function of ϕ with various $\Delta\phi$ for an energy transfer resolution $\Delta\varepsilon/\varepsilon = 0.01$.

Figure 7: Illumination criterion for a crystal monochromator on a pulsed source illustrating the need for high take-off angles at good resolution, and its consequence in favouring low incident energies for a typical d-spacing.

Figure 8: The flux at the sample position against neutron energy for 4 crystal arrangements: A - copper in transmission. B - out-of-plane focussed copper in reflection. C - out-of-plane focussed graphite. D - double graphite monochromator; and for a phased chopper (E).

Figure 9: Reduced energy transfer resolution $\Delta\varepsilon/E_1$ as a function of the scattered flight path for a chopper spectrometer with $d_1 = 10m$ and $d_3 = 1m$.

Figure 10: A schematic design of the MARS spectrometer on the SNS.

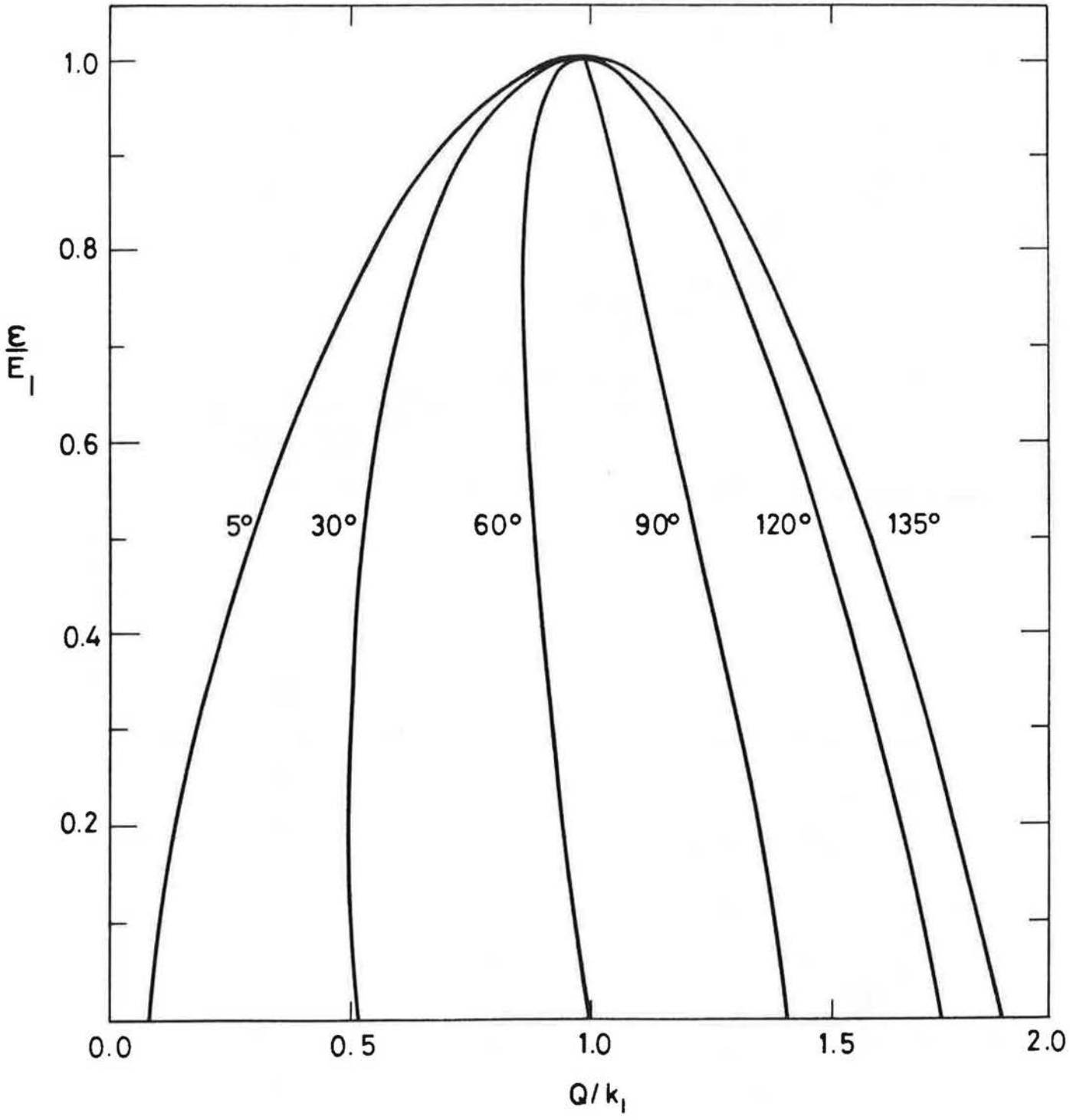
1.0
0.8
0.6
0.4
0.2
$\frac{\omega}{\omega_p}$
5°
30°
60°
90°
120°
135°
0.0
0.5
1.0
1.5
2.0
Q/k_1

FIGURE 1

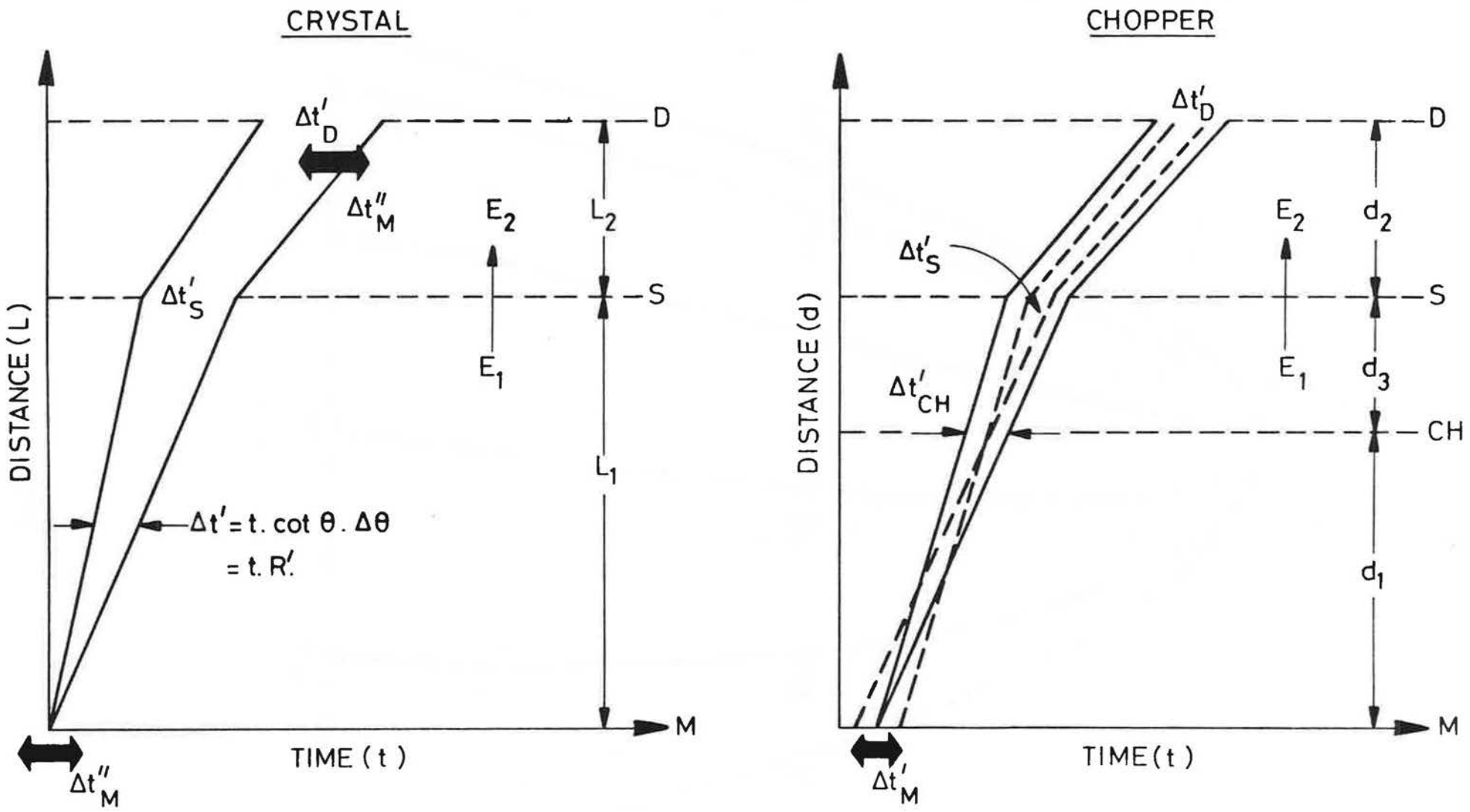
CRYSTAL
CHOPPER
DISTANCE (L)
DISTANCE (d)
TIME (t)
TIME (t)
D
S
M
CH
$\Delta t'_D$
$\Delta t''_M$
$\Delta t'_S$
$\Delta t'_{CH}$
$\Delta t''_M$
$\Delta t'_M$
E_2
E_1
L_2
L_1
d_2
d_3
d_1
$\Delta t' = t . \cot\theta . \Delta\theta$
$= t . R'$

FIGURE 2

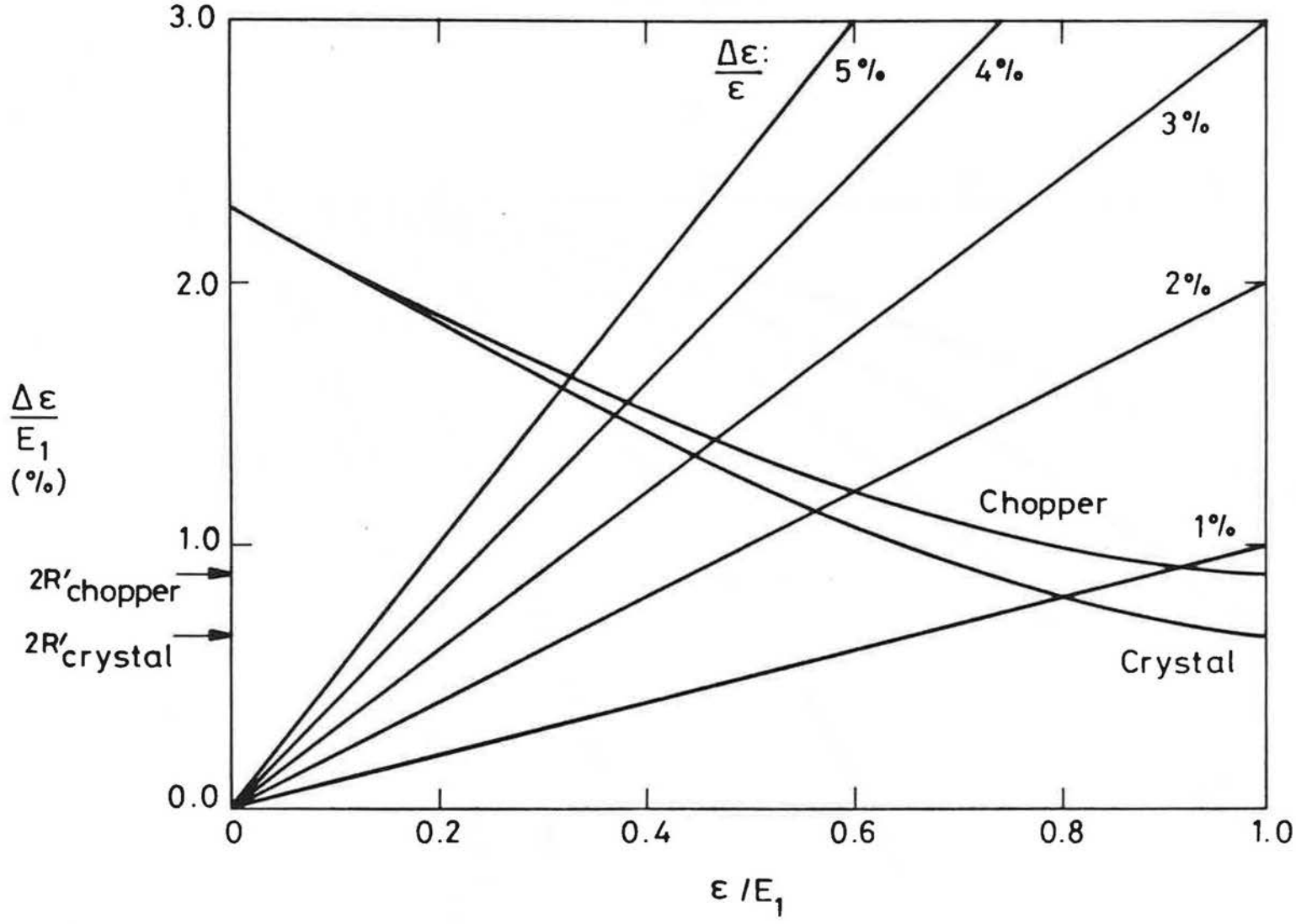
3.0
2.0
1.0
0.0
0
0.2
0.4
0.6
0.8
1.0
Δε/ε:
5%
4%
3%
2%
1%
Chopper
Crystal
Δε/E1 (%)
2R'chopper
2R'crystal
ε/E1

FIGURE 3

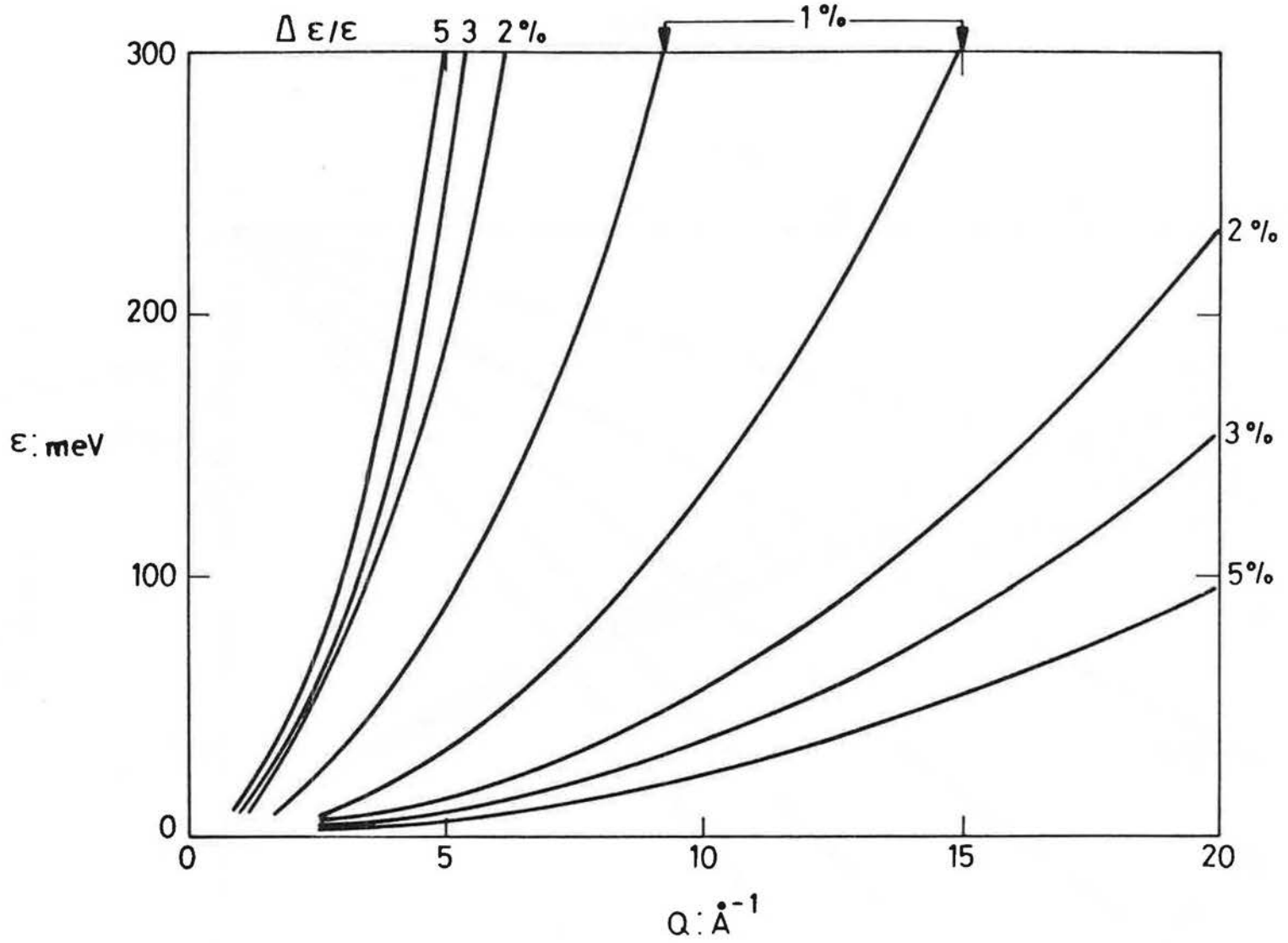

FIGURE 4

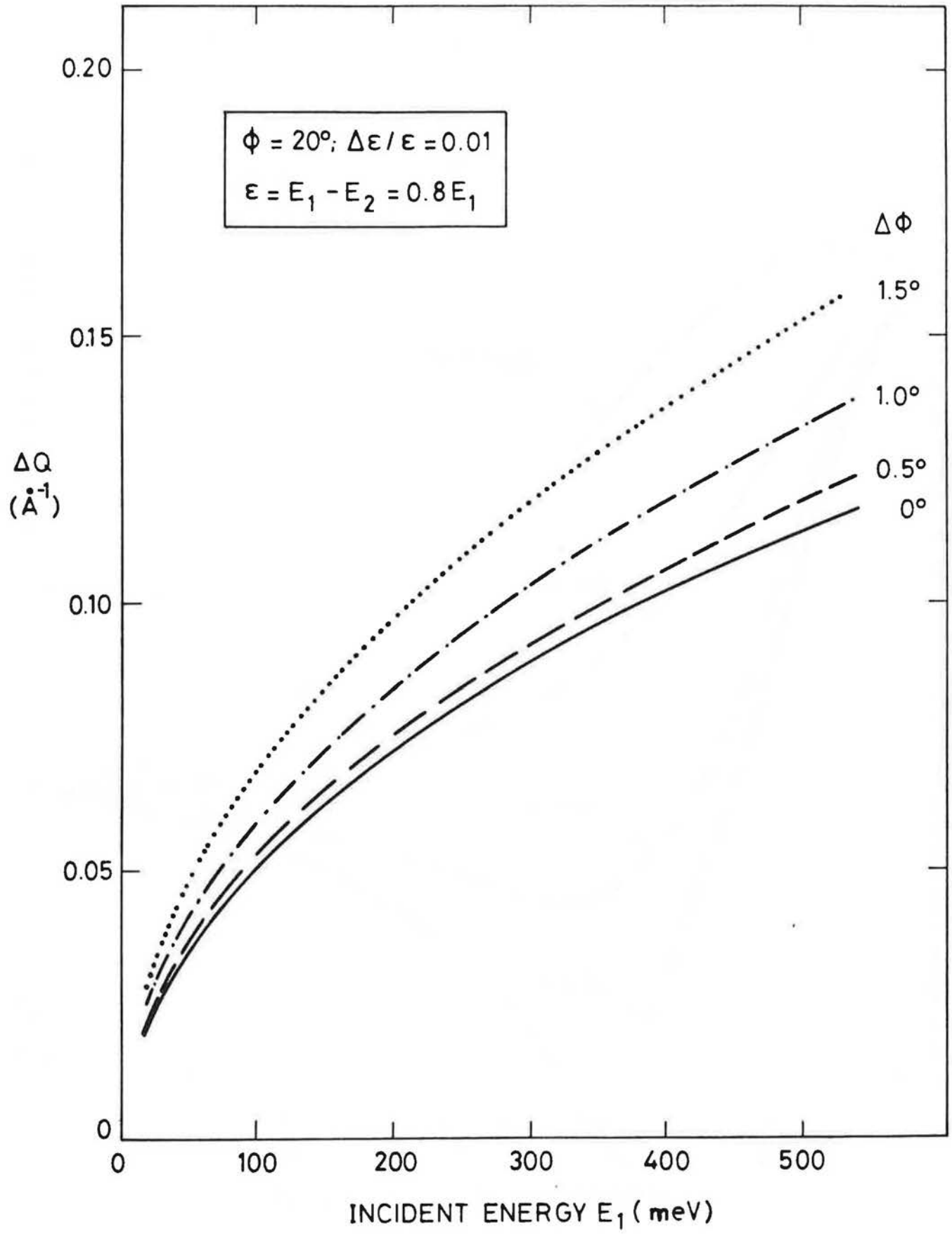
0.20
0.15
0.10
0.05
0
ΔQ
(Å⁻¹)
φ = 20°; Δε / ε = 0.01
ε = E1 - E2 = 0.8 E1
Δφ
1.5°
1.0°
0.5°
0°
0
100
200
300
400
500
INCIDENT ENERGY E1 (meV)

FIGURE 5

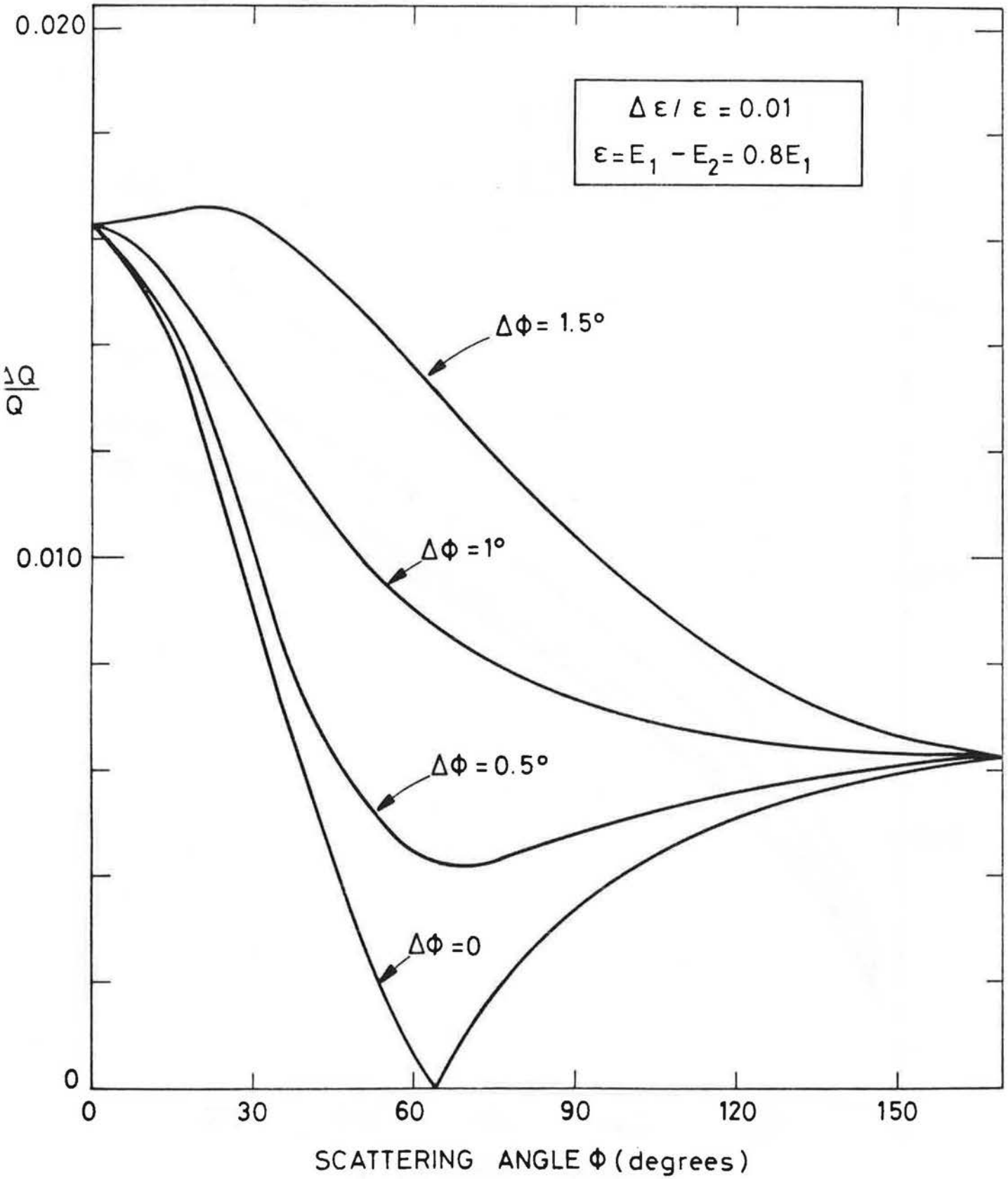
0.020
0.010
0
$\frac{\Delta Q}{Q}$
$\Delta\varepsilon/\varepsilon = 0.01$
$\varepsilon = E_1 - E_2 = 0.8E_1$
$\Delta\Phi = 1.5°$
$\Delta\Phi = 1°$
$\Delta\Phi = 0.5°$
$\Delta\Phi = 0$
0
30
60
90
120
150
SCATTERING ANGLE Φ (degrees)

FIGURE 6

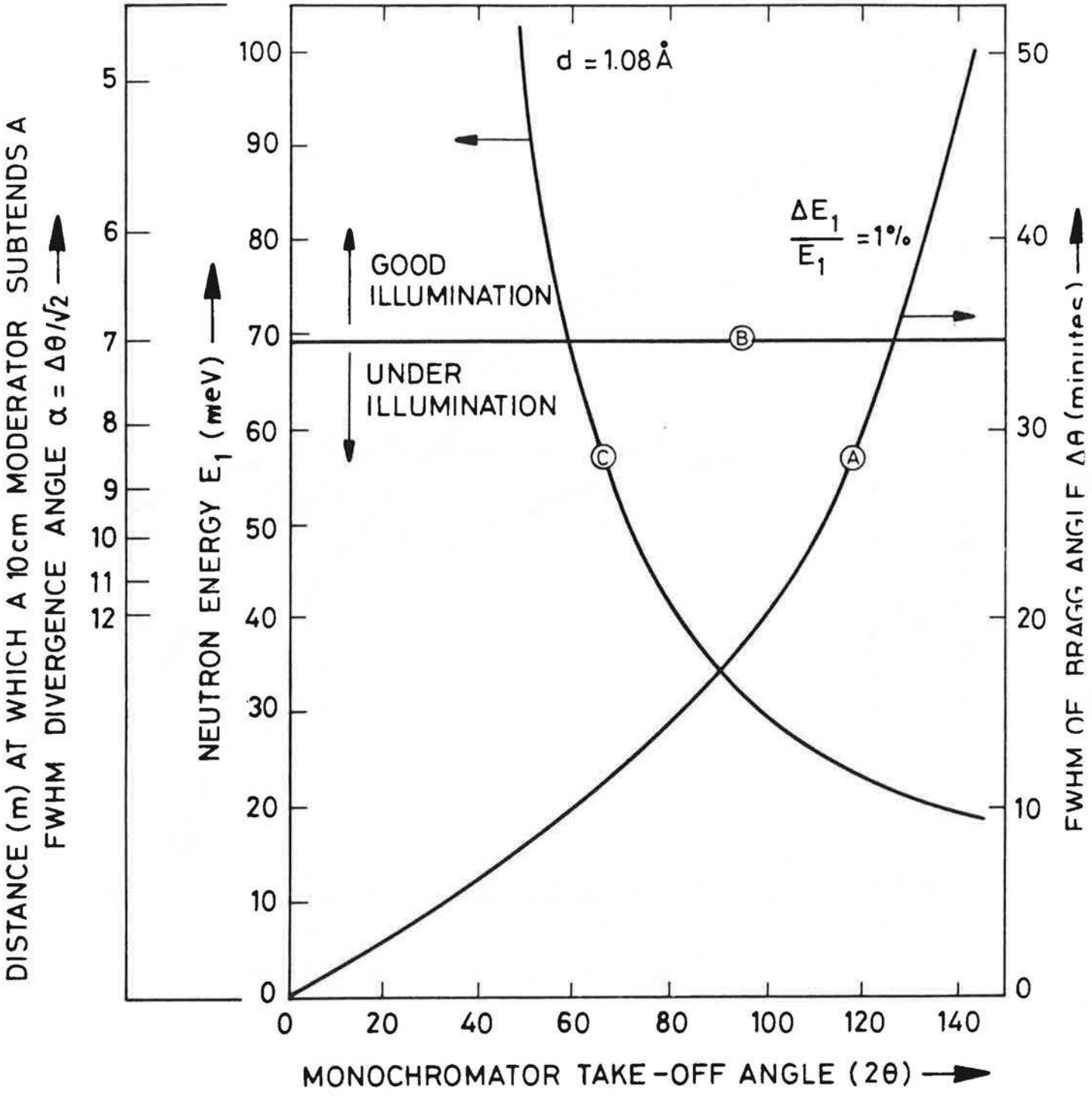
DISTANCE (m) AT WHICH A 10cm MODERATOR SUBTENDS A FWHM DIVERGENCE ANGLE α = Δθ/√2
NEUTRON ENERGY E1 (meV)
FWHM OF BRAGG ANGLE Δθ (minutes)
MONOCHROMATOR TAKE-OFF ANGLE (2θ)
d = 1.08 Å
ΔE1/E1 = 1%
GOOD ILLUMINATION
UNDER ILLUMINATION
A
B
C

FIGURE 7

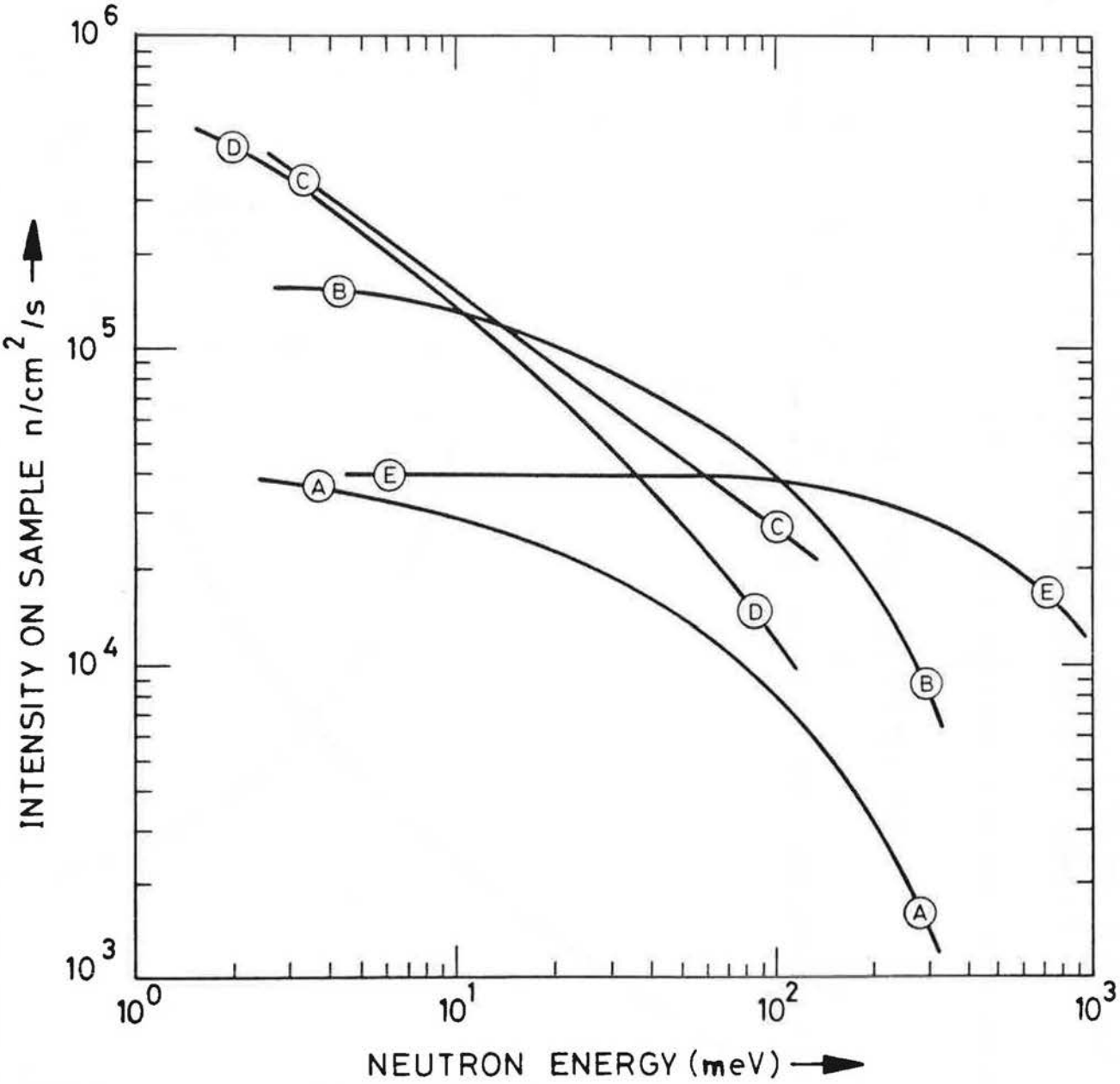
INTENSITY ON SAMPLE n/cm^2/s
10^6
10^5
10^4
10^3
10^0
10^1
10^2
10^3
NEUTRON ENERGY (meV)
A
B
C
D
E

FIGURE 8

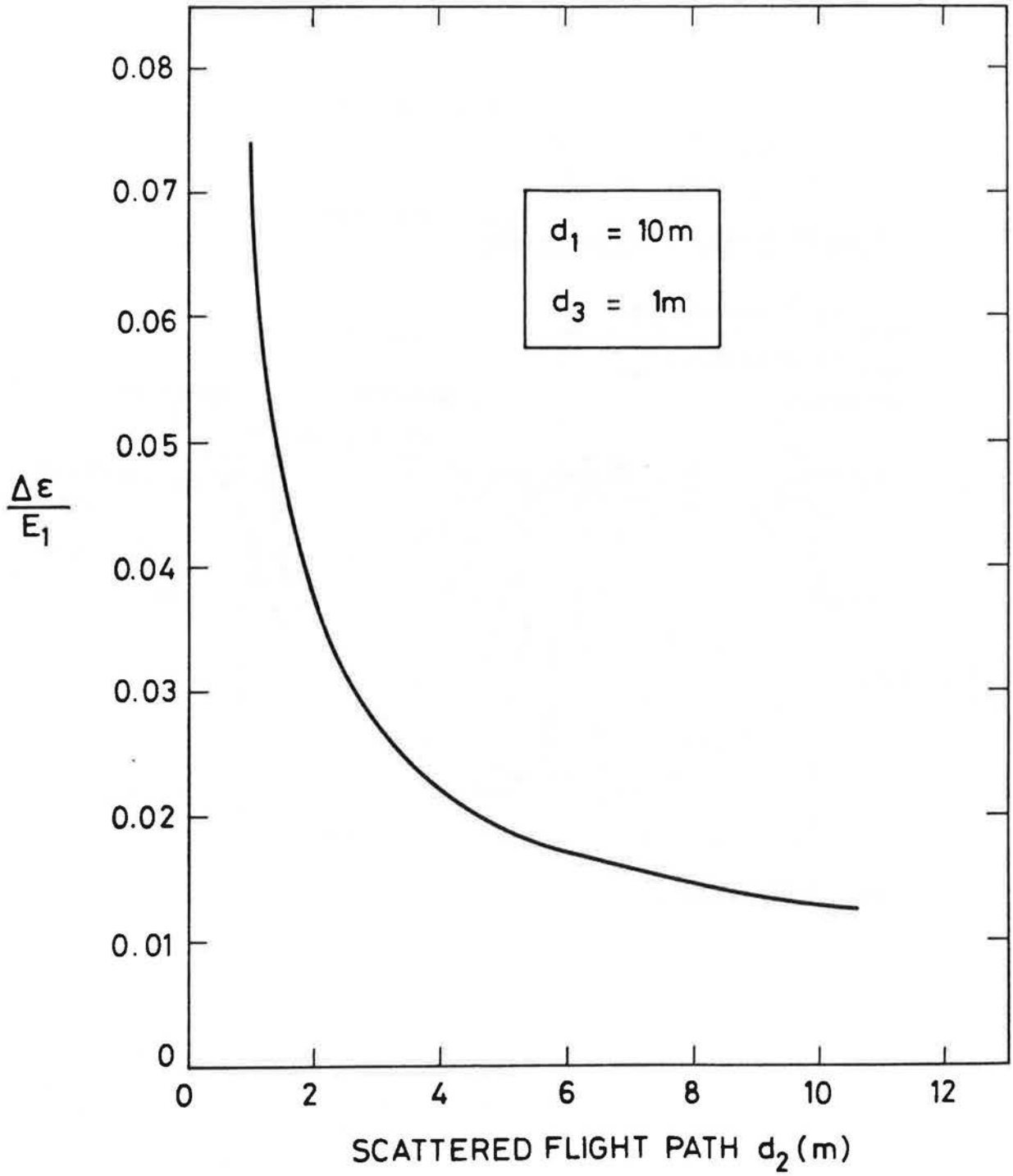
0.08
0.07
0.06
0.05
0.04
0.03
0.02
0.01
0
Δε/E1
d1 = 10m
d3 = 1m
0
2
4
6
8
10
12
SCATTERED FLIGHT PATH d2 (m)

FIGURE 9

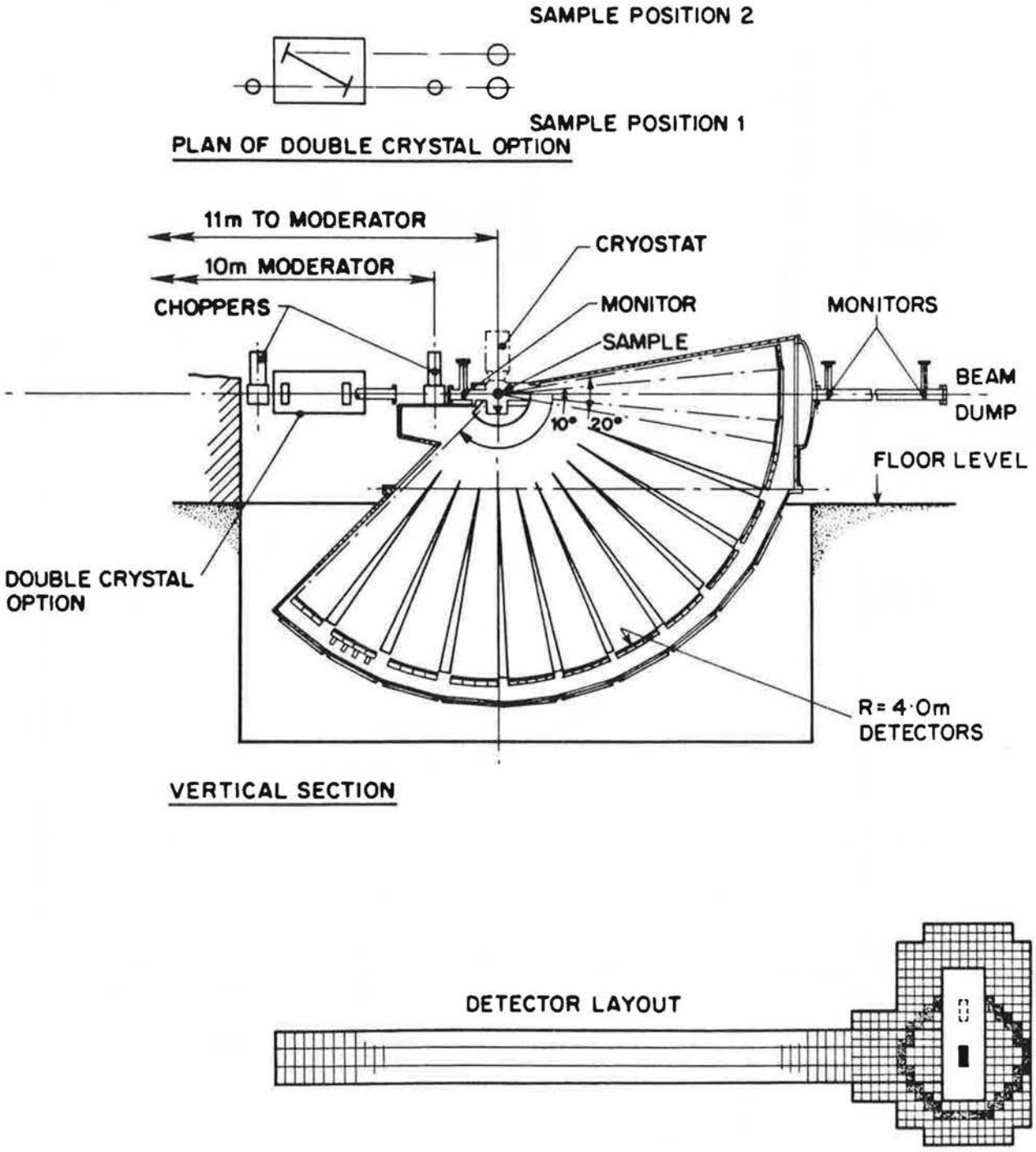
SAMPLE POSITION 2
SAMPLE POSITION 1
PLAN OF DOUBLE CRYSTAL OPTION
11m TO MODERATOR
10m MODERATOR
CHOPPERS
CRYOSTAT
MONITOR
SAMPLE
MONITORS
BEAM DUMP
10°
20°
FLOOR LEVEL
DOUBLE CRYSTAL OPTION
R = 4·0m DETECTORS
VERTICAL SECTION
DETECTOR LAYOUT

FIGURE 10